α–Catenin-dependent vinculin recruitment to adherens junctions is antagonistic to focal adhesions

Vidal Bejar-Padilla[a], Jolene I. Cabe[a], Santiago Lopez[a], Vani Narayanan[a], Mazen Mezher[b], Venkat Maruthamuthu[b], and Daniel E. Conway[a,c,d,*]

[a]Biomedical Engineering, Virginia Commonwealth University, Richmond Virginia 23284; [b]Mechanical & Aerospace Engineering, Old Dominion University, Norfolk Virginia 23529; [c]Biomedical Engineering, The Ohio State University; [d]Center for Cancer Engineering, Arthur G. James Comprehensive Cancer Center, The Ohio State University, Columbus Ohio 43210

ABSTRACT **Vinculin is a protein found in both focal adhesions (FAs) and adherens junctions (AJs) which regulates actin connectivity to these structures. Many studies have demonstrated that mechanical perturbations of cells result in enhanced recruitment of vinculin to FAs and/or AJs. Likewise, many other studies have shown "cross-talk" between FAs and AJs. Vinculin itself has been suggested to be a probable regulator of this adhesion cross-talk. In this study we used MDCK as a model system of epithelia, developing cell lines in which vinculin recruitment was reduced or enhanced at AJs. Careful analysis of these cells revealed that perturbing vinculin recruitment to AJs resulted in a reduction of detectable FAs. Interestingly the cross-talk between these two structures was not due to a limited pool of vinculin, as increasing expression of vinculin did not rescue FA formation. Instead, we demonstrate that vinculin translocation between AJs and FAs is necessary for actin cytoskeleton rearrangements that occur during cell migration, which is necessary for large, well-formed FAs. Last, we show using a wound assay that collective cell migration is similarly hindered when vinculin recruitment is reduced or enhanced at AJs, highlighting that vinculin translocation between each compartment is necessary for efficient collective migration.**

Monitoring Editor
Alpha Yap
University of Queensland

Received: Mar 2, 2022
Revised: Jul 11, 2022
Accepted: Jul 25, 2022

INTRODUCTION

Adherens junctions (AJs) and focal adhesions (FAs) are macromolecular protein assemblies localized in the cell membrane at cell–cell and cell–matrix interfaces, respectively. By forming the mechanical link between the actomyosin network within the cell and the external environment, AJs and FAs withstand the forces generated by the actomyosin network within the cell and forces generated externally by the surrounding environment (Humphries *et al.*, 2007; Vasquez and Martin, 2016). To dynamically sense and respond to this bidirectional force transmission, AJs and FAs recruit mechanosensitive adaptor proteins that mechanically couple transmembrane adhesion proteins to the intracellular actomyosin network. The recruitment and activity of these adaptor proteins, including cytoskeletal association, have been shown to be regulated by mechanical and biochemical signals (Campbell and Humphries, 2011; Geiger and Yamada, 2011; Mui *et al.*, 2016; Vasquez and Martin, 2016; De Pascalis and Etienne-Manneville, 2017). These adaptor proteins regulate AJ and FA dynamics, including adhesion strength and turnover. Together, the wide milieu of proteins that act at AJs and FAs sensitize these structures to mechanical signals. This mechanosensitivity allows cells to integrate and respond to cues received during dynamic physiological phenomena such as collective cell migration (De Pascalis and Etienne-Manneville, 2017).

While the fundamental assemblies comprising AJs and FAs are strikingly distinct in their biomolecular makeup and subcellular localization, studies of mechanical signaling within cells have shown that information can be communicated between cell–cell and cell–matrix interfaces via changes in the tensile actin network, frequently referred to as "cross-talk" (Weber *et al.*, 2012; Mui *et al.*, 2016). An increase

This article was published online ahead of print in MBoC in Press (http://www.molbiolcell.org/cgi/doi/10.1091/mbc.E22-02-0071) on August 3, 2022.

*Address correspondence to: Daniel E. Conway (conway.362@osu.edu).

Abbreviations used: AJ, adherens junction; BSA, bovine serum albumin; CA, conformationally active; ECM, extracellular matrix; EMT, epithelial-mesenchymal transition; FA, focal adhesion; KO, knockout; MDCK, Madin-Darby canine kidney; WT, wild-type.

in substrate stiffness sensed by FAs, for example, enhances the force-dependent activation and recruitment of adaptor proteins at AJs (Seddiki *et al.*, 2018). More recently, it has been shown that biochemical signals can be transmitted between AJs and FAs via shared adaptor proteins (Mui *et al.*, 2016). Namely, the mechanosensitive adaptor protein vinculin has been shown to regulate adhesion dynamics at both the cell–cell and the cell–matrix interface (Bays and DeMali, 2017). At AJs, the cytosolic domain of the transmembrane protein cadherin interacts with α-catenin and β-catenin to form the cadherin–catenin complex. This complex forms the minimum mechanical link between neighboring cells and the internal actin cytoskeleton via cadherin's transinteraction with cadherins on the surface of neighboring cells and α-catenin's interaction with F-actin. Following an increase in intercellular tension, α-catenin undergoes a conformational change that exposes a cryptic binding site for vinculin, allowing vinculin to be recruited to AJs (Yonemura *et al.*, 2010; Sumida *et al.*, 2011). It is worth noting that vinculin also interacts with β-catenin at AJs, though this interaction appears to be force independent (Peng *et al.*, 2012). Together, α-catenin and vinculin cooperatively recruit F-actin to the cadherin–catenin complex. Numerous studies have shown that perturbing the force-dependent recruitment of vinculin to the cadherin–catenin complex reduces the sensitivity of AJs to changes in intercellular tension, alters cell–cell adhesion dynamics, and regulates barrier function. (Yonemura *et al.*, 2010; Matsuzawa *et al.*, 2018; Noethel *et al.*, 2018; Seddiki *et al.*, 2018; Koirala *et al.*, 2021; Monster *et al.*, 2021). Vinculin plays a similar role at FAs following its recruitment by talin, a protein which complexes with the transmembrane receptor integrin and other adaptor proteins like paxillin (Humphries *et al.*, 2007; Del Rio *et al.*, 2009; Campbell and Humphries, 2011). Once recruited, vinculin links the FA complex to the actin cytoskeleton and regulates the activity of other FA proteins. Though vinculin is not required for FA formation, perturbing recruitment of vinculin to FAs has been shown to inhibit the generation of traction force needed to enable cell migration and alters cell–matrix adhesion dynamics (Huttenlocher and Horwitz, 2011; Carisey *et al.*, 2013; Mertz *et al.*, 2013; Bays and DeMali, 2017).

Since vinculin has been identified as an important regulator of both AJ and FA dynamics, it represents a probable regulator of cross-talk between these adhesions. Notably, vinculin has been shown to translocate from FAs to AJs following assembly of AJs and in response to cyclic stretch, with this effect correlating with a significant reduction in FA coverage (Noethel *et al.*, 2018). Blocking this translocation to AJs with a mutant of α-catenin lacking the vinculin binding domain inhibited the alignment of actin fibers in response to stretch, an important indicator of cellular sensitivity to strain. These observations suggest that the translocation of vinculin from FAs to AJs transfers mechanosensitivity to AJs, and that this is important for sensitizing the collective epithelium to mechanical stimulus (Noethel *et al.*, 2018). Additionally, it was shown that enhancing vinculin recruitment to AJs inhibits collective cell migration in epithelial monolayers by inhibiting anisotropic force transmission necessary for efficient communication of mechanical cues between migrating cells (Matsuzawa *et al.*, 2018). However, the role of vinculin translocation to AJs on regulation of FAs is still largely unclear.

Given the role of vinculin in mechanosensitivity at both types of cell adhesions, it stands to reason that force-dependent translocation of vinculin to AJs may create changes in intercellular tension that induce remodeling of FAs. As previously mentioned, an increase in substrate stiffness at the cell–matrix interface strengthens intercellular junctions, suggesting that mechanical homeostasis must be achieved at both interfaces via cooperative remodeling (Seddiki *et al.*, 2018). However, an antagonistic relationship has also been observed, where increased mechanical stimulation at one interface weakens adhesion strength in the other (Mui *et al.*, 2016). Since both models appear to be true under different experimental conditions, cellular integration of complex biomechanical signals likely involves both cooperative and antagonistic remodeling. Understanding the role of vinculin translocation in response to external mechanical stimulus may help to further elucidate how cell–cell and cell–ECM adhesions coordinate remodeling at distinct cellular interfaces. To study this hypothesis, we developed Madin-Darby canine kidney (MDCK) cells with either enhanced or reduced α–catenin-dependent vinculin recruitment to AJs. We observed impaired FA formation in response to enhanced or reduced vinculin recruitment to AJs. The disrupted FA morphology was, however, not rescued by vinculin overexpression, indicating that the AJ to FA cross-talk is not likely regulated by a limited cytosolic "pool" of vinculin. However, FA morphology in cells with enhanced vinculin recruitment to AJs was rescued with calcium depletion, indicating that AJs directly regulate FA dynamics. Additionally, we observed that both enhancement and reduction of vinculin recruitment to AJs equally inhibited collective cell migration, indicating that vinculin translocation between AJs and FAs is necessary for collective migration. We propose that α–catenin-dependent vinculin recruitment to AJs is involved in coordinating the formation and disassembly of FAs during collective cell migration via control of subcellular force transmission between the cell–cell and the cell–matrix interface.

RESULTS

Rescue of α-catenin knockout cells with α-catenin mutations to perturb vinculin recruitment to AJs

To perturb vinculin translocation between AJs and FAs, mutants of α-catenin with modifications to the vinculin binding site were developed in MDCK II cells based on previously published work. α-Catenin KO cells were rescued with either α-catenin-WT, α-catenin L344P (Peng *et al.*, 2012), which was shown to inhibit recruitment of vinculin to AJs, or the α-catenin conformationally active (CA) mutant, which was shown to enhance recruitment of vinculin to AJs (Matsuzawa *et al.*, 2018). All α-catenin mutants included an N-terminal mCherry fluorescent tag. Schematics of α-catenin mutants are shown in Figure 1A. Western blotting was performed to confirm the knockout and rescue of α-catenin in all cell-lines (Figure 1B). To evaluate α–catenin-dependent changes in vinculin recruitment to AJs, mutant cell lines were stained for α-catenin and vinculin (Figure 1C). As expected, vinculin was not observed at cell–cell contacts in α-catenin KO cells. WT, L344P, and CA mutants rescued vinculin recruitment to AJs. Quantification of vinculin recruitment to AJs relative to average cytoplasmic signal showed that vinculin recruitment to AJs was enhanced in CA cells and reduced in L344P cells relative to WT (Figure 1D).

Perturbing vinculin recruitment to AJs alters FA abundance and distribution in migrating cells

To evaluate the role of vinculin recruitment to AJs in regulating FAs, subconfluent colonies of cells were stained for α-catenin, vinculin, and the FA markers paxillin (Figure 2A) and talin (Supplemental Figure S1). Images were collected at the migrating edge of the monolayer. Instead of focusing on the apical region of the cell populated by AJs as was done in Figure 1, images were taken at the basal region of the cell to better visualize FAs. Two distinct populations of vinculin were observed at this plane, one colocalized with α-catenin at basally positioned AJs and the other population saturating the cell–matrix interface in scattered foci, a distribution characteristic of FAs. In α-catenin WT cells, vinculin distribution was strongly biased toward FAs, with little to no vinculin observed at cell–cell contacts.

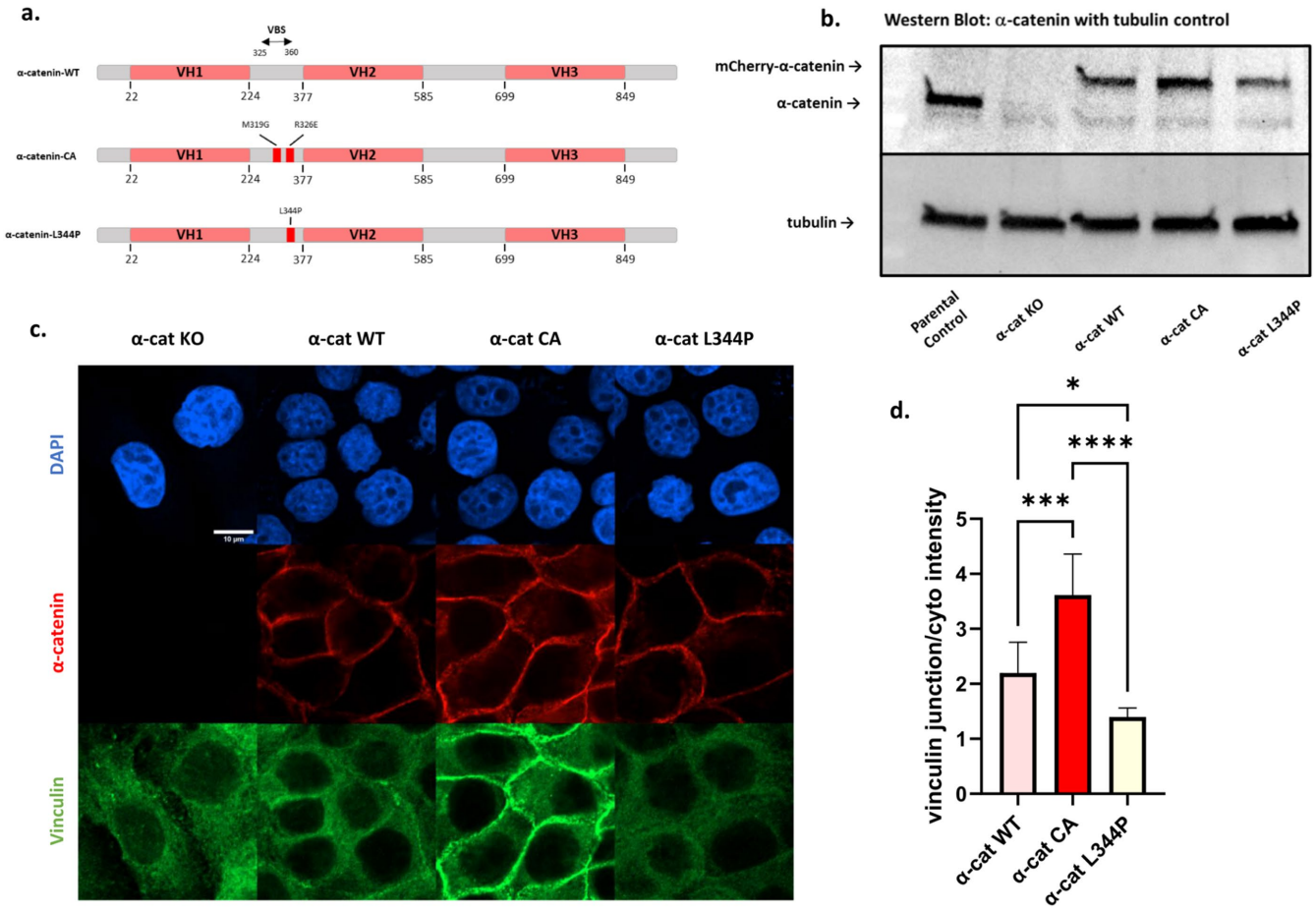

FIGURE 1: Development of α-catenin mutants perturbing vinculin recruitment to AJs. (A) Schematic showing the positions of α-catenin mutations in rescue cell lines. (B) Western blot of α-catenin rescue cell lines blotted for α-catenin. (C) Confluent cell monolayers expressing α-catenin mutants were stained for vinculin. Scale bar represents 10 μm (D) Quantification of vinculin recruitment to cell–cell contacts. Vinculin intensity was measured at cell–cell contacts and at three randomly selected points within the cytoplasm. Ratios of junctional and average cytoplasmic vinculin intensity were plotted; $n = 6$ images from two independent experiments. One-way ANOVA with Tukey comparison test was performed to determine significance.

FAs were abundant and distributed across the cell–matrix interface. This phenotype was observed in both cells at the leading edge (leader cells) of the monolayer and cells without free edges (follower cells). By contrast, vinculin recruitment to AJs persisted in all observed α-catenin CA cells. Strikingly, while FAs were detected in CA leader cells, follower cells exhibited a reduction in FA abundance. When compared with WT, L344P cells exhibited similar amounts of FAs in both leader and follower cells, though there was an apparent increase in abundance of small FAs.

To quantify these phenotypes, a previously developed automated approach for labeling FAs (Horzum *et al.*, 2014) was employed. Quantification of FAs revealed that both CA and L344P cells exhibited an overall reduction in FA number per cell, with the difference being most dramatic in CA cells (Figure 2C). It is likely that the discrepancy between the observed phenotype and the quantified reduction in FA number seen in L344P cells is accounted for by the higher proportion of small FAs that are not detected by this automated analysis (see *Methods* and Supplemental Figure S2). Substantiating a functional consequence for this drop in FAs, CA cells had significantly smaller areas at the edges of the cell monolayer when compared with WT (Figure 2B). On average, L344P cell areas were of an intermediate value between α-catenin WT and CA cells, though this result was not statistically significant. Importantly, in confluent conditions, there were no differences in average cell area across the three cell types (Figure 2B). The number of detectable FAs per a given area, or FA density, was also quantified, with CA and L344P cells exhibiting smaller densities on average (Figure 2D). Combined, the FA defects observed in CA and L344P cells suggests that perturbing vinculin to AJs results in impairment of the assembly of large FAs during migration, likely accounting for the failure of α-catenin CA cells to effectively spread out. In all three cell lines, vinculin remains present in paxillin-labeled (Figure 2A) and talin-labeled FAs (Supplemental Figure S1), indicating that FAs in all three cell lines contain vinculin.

To determine whether α-catenin CA cells (which exhibited the most significant impairment of FAs) have altered traction forces, we examined the traction forces exerted by small colonies of MDCK expressing CA or WT α-catenin (Figure 2E). Traction force microscopy revealed no significant differences between WT or CA (Figure 2F). Thus, while the CA mutant induces a significant impairment FA formation as evidenced by immunostaining, overall traction forces were not reduced.

FA disruption is rescued in response to AJ disruption but not overexpression of vinculin

The distinct decrease in FA abundance observed in CA cells, particularly that of follower cells (Figure 2A), suggested a hypothesis

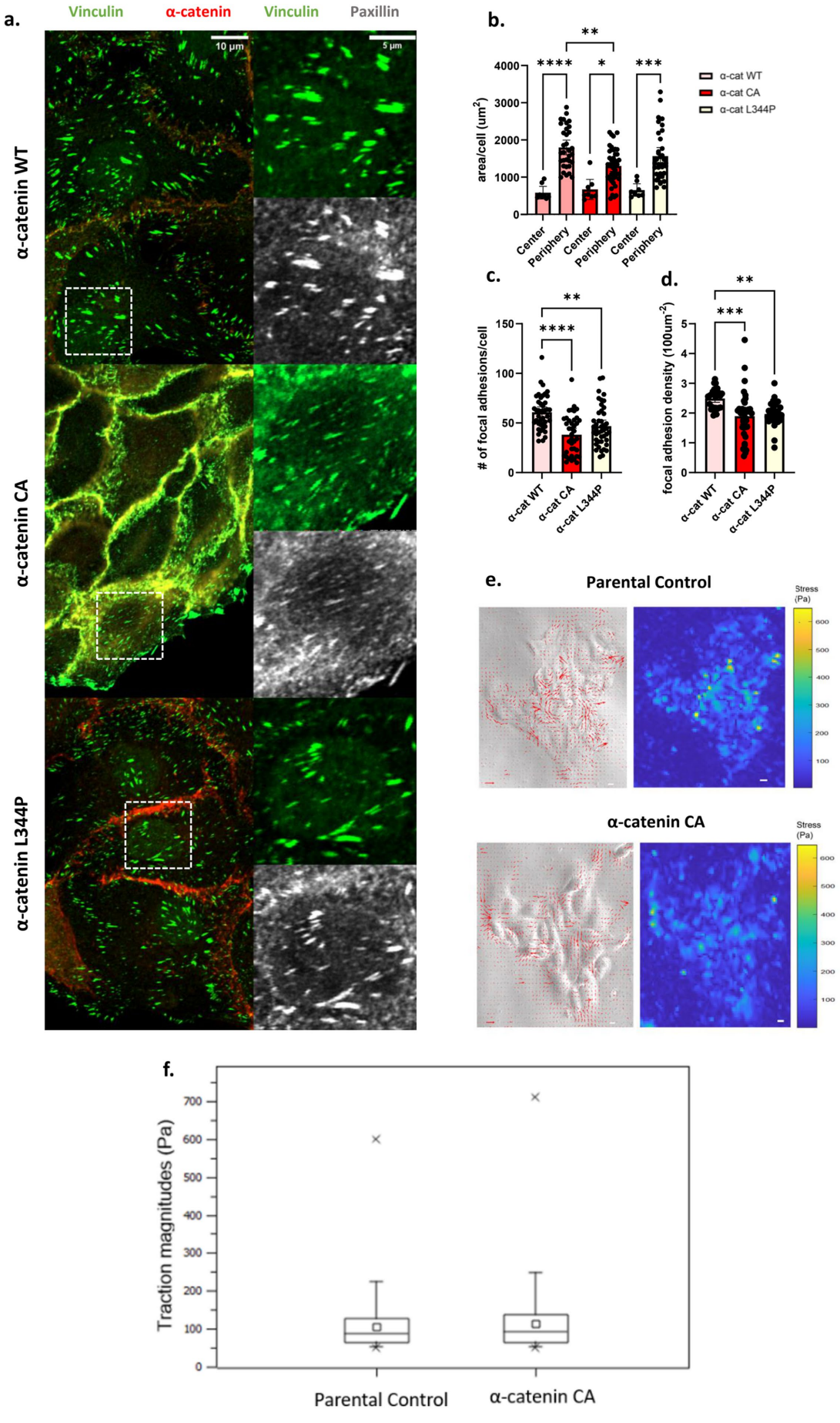
a.
Vinculin
α-catenin
Vinculin
Paxillin
10 μm
5 μm
α-catenin WT
α-catenin CA
α-catenin L344P
b.
area/cell (um²)
α-cat WT
α-cat CA
α-cat L344P
Center
Periphery
c.
# of focal adhesions/cell
d.
focal adhesion density (100um⁻²)
e.
Parental Control
α-catenin CA
Stress (Pa)
f.
Traction magnitudes (Pa)
Parental Control
α-catenin CA

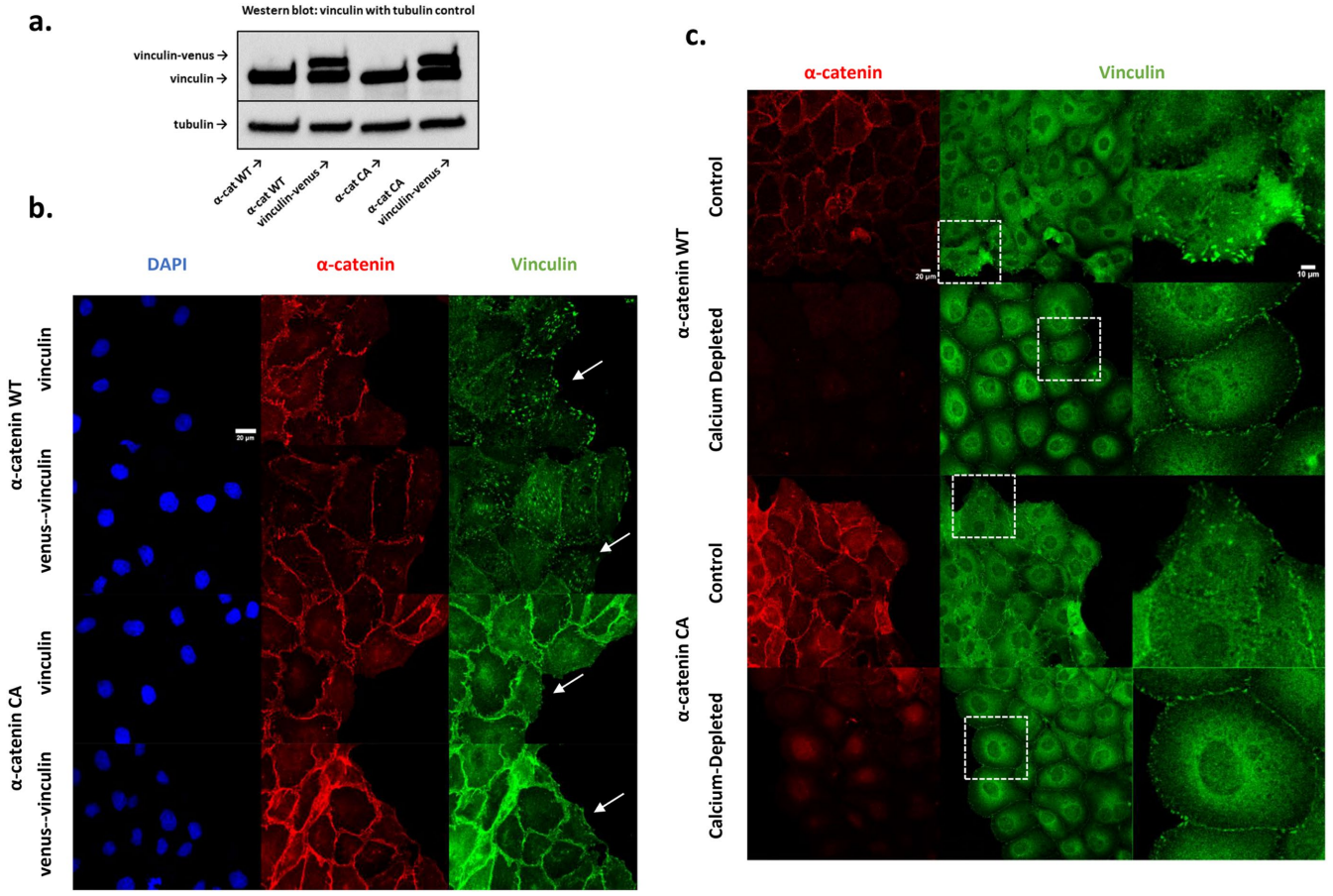

FIGURE 3: Impairment of FAs depends on stability of cell–cell contacts but not on availability of vinculin. (A) Western blot of vinculin in α-catenin mutants showing overexpression of vinculin-venus (B) Vinculin localization in vinculin-overexpressing cells was analyzed with immunofluorescent staining. White arrows point to vinculin foci at FAs (C) Vinculin localization in calcium-depleted cells was analyzed with immunofluorescent staining. White boxes label expanded region in following column.

that vinculin recruitment to AJs is antagonistic to the formation of FAs. We sought to examine two possible mechanisms as to why enhancing vinculin recruitment to AJs resulted in altered FAs: 1) a limited "pool" of vinculin results in insufficient vinculin molecules to be effectively incorporated at both AJs and FAs or 2) formation of vinculin-positive AJs directly alters FA dynamics. To test the first mechanism, we sought to dramatically increase the level of vinculin protein expression to determine if additional molecules of vinculin would rescue FA formation in CA cells. Importantly, expressing vinculin-venus in MDCK did not affect endogenous vinculin expression (Figure 3A); thus in total these cells had a much higher expression level of vinculin. CA cells overexpressing vinculin also had impaired FA formation that was similar to CA cells without vinculin overexpression (Figure 3B).

To test the second potential mechanism of direct antagonism of FAs by AJs, we examined if AJ disruption by calcium depletion would restore FA formation. Calcium depletion resulted in disruption of AJs, as indicated by the lack of α-catenin staining at cell–cell interfaces (Figure 3C). In WT calcium-depleted cells, FAs in cells at the edge of the monolayer reorganized to populate the periphery of the cell, with little to no FAs observed further within the boundaries of the cell (Figure 3C). Importantly, FA distribution in calcium-depleted CA cells mirrored that seen in calcium-depleted WT cells. This result shows that in the absence of α-catenin at intercellular contacts, CA cells are able to form FAs in a way that recapitulates what is seen in WT cells, a result that supports the hypothesis that recruitment of vinculin to AJs specifically is directly antagonistic to FAs.

FIGURE 2: Enhancing vinculin recruitment to AJs alters FA morphology and density of migrating cells. (A) Periphery of cell monolayers expressing α-catenin mutants were stained for vinculin and the FA markers paxillin and talin. Dotted white boxes indicate zoomed-in region. (B) Quantification of average cell area; $n = 8$ images from two independent experiments for confluent condition; $n \geq 33$ images from six independent experiments for periphery condition. (C) Quantification of average FA number per cell at periphery of monolayer; $n \geq 39$ images from six independent experiments (D) Quantification of FA density. $n \geq 28$ images from six independent experiments. One-way ANOVA with Tukey comparisons was performed for all statistical analyses. (E) Phase image of cell islands with traction stress vectors (red vectors) superimposed and heat map representation of the traction stress of the cell island. (F) Box plot comparison of the traction magnitude distribution for parental control and α-catenin-CA cell islands. Statistical properties are as follows: mean (open square), box (25/75% quartile), whisker (5/95% quartile), diagonal cross (maximum/minimum). No statistical difference ($p > 0.05$) was observed for traction magnitudes between WT and CA conditions.

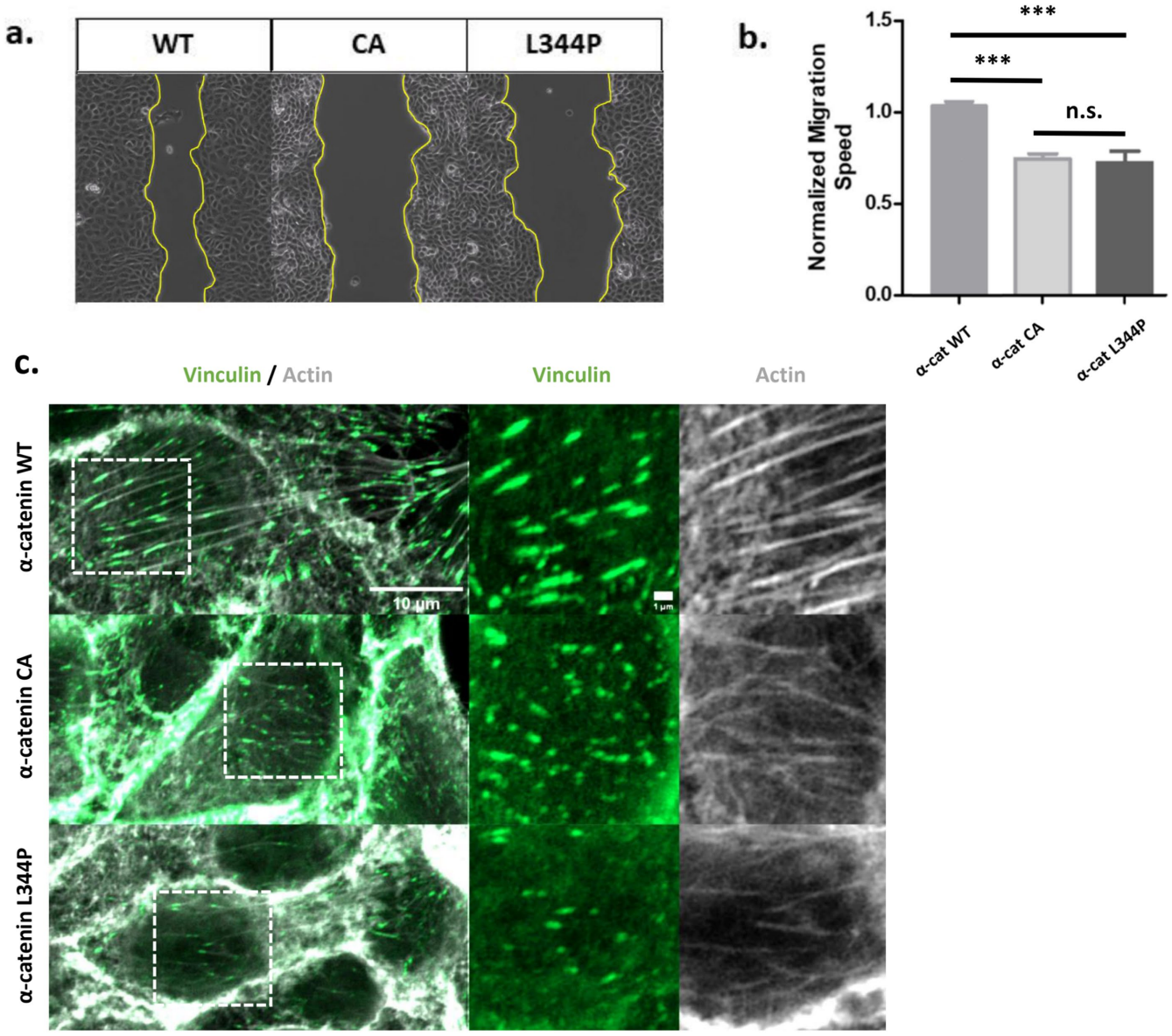

FIGURE 4: Inhibited collective cell migration in α-catenin mutants coincides with altered FA and actin fiber morphology at leading edge of migrating monolayer. (A) Representative image of cell monolayers following 6 h of collective migration. Leading edge is highlighted in yellow. (B) Quantification of rate of migration normalized to α-catenin WT migration rate. Migration of monolayers was quantified with image analysis. (C) Monolayers were fixed 6 h after start of migration and stained for vinculin and actin.

L344P and CA α-catenin similarly impair collective cell migration

Next, we wanted to probe the functional consequence of perturbed FA remodeling that arises as a result of impaired vinculin translocation. As previously mentioned, force-dependent recruitment of vinculin to AJs has been shown to mediate intercellular force transmission during collective cell migration (Matsuzawa *et al.*, 2018). However, the role of vinculin translocation to AJs in regulating FAs and their associated contractile machinery at the cell–matrix interface is not well understood. For this reason, we performed a collective cell migration assay and compared the phenotype of vinculin-labeled FAs and their associated actin cytoskeleton in cells at the leading edge of migrating monolayers.

Cell monolayers were allowed to migrate into a cell-free space over the course of 6 h (Figure 4A). Collective migration rate quantification showed significant impairments to CA and L344P collective migration speed when compared with WT (Figure 4B). This result highlights that either enhancement or inhibition of vinculin recruitment to AJs has a similar reduction in the rate of migration. To visualize FAs and their associated actin fibers during directional collective migration, cell monolayers were allowed to migrate for 6 h prior to fixation and staining. Both CA and L344P cells had impaired FA formation (Figure 4C) consistent with results seen in Figure 2, D–E. Actin stress fibers in migrating WT cells were abundant and engaged with both intercellular junctions and cell–matrix adhesions. In contrast, actin in migrating CA and L344P cells remained primarily concentrated at the cell cortex (Figure 4C). Time-lapse imaging was performed for migrating WT, CA, and L344P cells expressing vinculin-venus to visualize FAs and the associated actin network. Slower rates of FA formation and disassembly were observed for both CA

and L344P cells during migration (Supplemental Movies S1–S3). Membrane protrusion size and frequency appeared to be attenuated in CA and L344P cells when compared with WT as well.

DISCUSSION

In this work we directly compared two existing α-catenin mutations, L344P (inhibition of vinculin recruitment) and CA (M319G/R326E, enhancement of vinculin recruitment), to understand how changes in vinculin recruitment to cell–cell adhesions modulate epithelial cell behavior. Although the effects of these mutants have been examined in epithelial cells in a number of prior studies (Peng *et al.*, 2012; Yao *et al.*, 2014; Matsuzawa *et al.*, 2018; Seddiki *et al.*, 2018; Sakakibara *et al.*, 2020; Yang *et al.*, 2022), our work is the first to simultaneously compare CA and L344P α-catenin mutations, including a careful examination of how these mutations affect FAs. The major finding of this study is that enhancement or inhibition of α–catenin-dependent vinculin recruitment to cell–cell adhesions antagonizes the formation of cell–matrix adhesions, resulting in an impaired rate of collective cell migration and defective reorganization of the actin cytoskeleton during migration. Restoration of normal FA phenotype in CA cells as result of AJ disruption (Figure 3C) indicates that this antagonism is labile. Thus, it appears the ability of vinculin to move between cell–cell and cell–ECM adhesions is a critical component of collective cell migration.

In this context, the specific mechanism by which perturbed vinculin translocation antagonizes FA formation remains unclear, though our findings provide several important insights. Based on previous studies highlighting the importance of vinculin translocation between the cell–cell and the cell–matrix interface for cellular sensitivity to external forces (Noethel *et al.*, 2018), we propose that impairment of FAs is a consequence of defective force transmission between cell–cell and cell–matrix adhesions. In CA cells, enhanced vinculin recruitment to AJs prevents traction force generated in leader cells from being effectively transmitted to follower cells across intercellular contacts (Matsuzawa *et al.*, 2018). In L344P cells, inhibition of vinculin recruitment to AJs inhibits force-dependent recruitment of actin to AJs and alters cadherin-associated contractility, illustrating defective mechanical signaling at AJs (Seddiki *et al.*, 2018; Yang *et al.*, 2022). Here we illustrate impaired FA formation (Figure 2, D and E) and actin reorganization (Figure 4C) in migrating cells with perturbed vinculin translocation, suggesting that the mechanical polarization generated by the transmission of traction forces across intercellular contacts is necessary for proper FA assembly.

While CA and L344P cells share altered force transmission at cell–cell contacts, their unique FA distributions (Figure 2A) suggest that the mechanism causing failure of FA assembly is also unique. It stands to reason that in CA cells, engagement of the actomyosin network at cell–cell interfaces resulting from enhanced vinculin recruitment limits the network's association with the cell–matrix interface (Noethel *et al.*, 2018), preventing forces transmitted from neighboring cells from being effectively levied at this interface. Evidence against an alternative hypothesis in which sequestration of vinculin at AJs leaves insufficient vinculin molecules for FAs is provided by the result that vinculin overexpression does not rescue impaired FA formation (Figure 3B). In L344P cells, defective mechanical signaling at intercellular contacts appears to have the functionally similar effect of attenuating force transmission from cell–cell contacts to the cell–matrix interface as determined by similarly defective FA formation in these cells.

Although CA cells exhibited the most dramatic defects in FA formation and cell spreading (Figure 2, A–D), traction force measurements suggest that these cells do not have reduced traction force (Figure 2, E and F). Although this result may seem contradictory, as described previously, it is likely that proper intercellular and interadhesion transmission of these equivalent traction forces is required for proper FA formation. Alternatively, it is possible that although the FA number is reduced, these FAs transmit higher loads, thereby resulting in equivalent traction forces. These data are also supported by the observation that loss of vinculin had minimal effects on cell–ECM adhesion strength in fibroblasts (Gallant *et al.*, 2005). Last, we note there are significant differences in ECM stiffness between immunostaining in Figure 2A (cells grown on glass) and traction force microscopy in Figure 2B (cells grown on silicone). Vinculin recruitment to both FAs and cell–cell adhesions has already been shown to be dependent on substrate stiffness (Zhou *et al.*, 2017; Seddiki *et al.*, 2018). It will be interesting to see if vinculin translocation between cell–cell and cell–matrix adhesions is important for cellular sensing of substrate stiffness.

A surprising finding of this work is that α-catenin CA and L344P each exhibited a similar reduction in migration speeds as compared with cells expressing WT α-catenin (Figure 4, A and B). Reduced collective migration velocity has already been reported for α-catenin CA cells, which was attributed to impaired directional cooperativity as a result of altered intercellular force transmission (Matsuzawa *et al.*, 2018). Although we are the first to report delayed collective migration speeds in α-catenin L344P cells in a wound-healing context, we note that another study previously observed decreased movement correlation in constrained cell collectives, as well as decreased cell contact lifetimes (Seddiki *et al.*, 2018). It is tempting to speculate that our observation of reduced FA formation in migrating CA and L344P cells (Figures 2A, 3B, and 4C) simultaneously results from and contributes to deficient mechanical polarization of these cells toward the axis of migration. Finally, our findings are additional evidence to support the hypothesis that epithelial cells can have either, but not both, mechanically strong cell–cell junctions or mechanically strong cell–ECM adhesions (Scott *et al.*, 2020), for example, during EMT cells transition from a state of higher cell–cell forces to a state of higher ECM forces (Gomez *et al.*, 2010; Narayanan *et al.*, 2020; Scott *et al.*, 2020). Taken together, our data in this manuscript indicate that collective cell migration during wound healing requires translocation of vinculin between cell–cell and cell–matrix adhesions. The effect of this translocation is likely most important for mechanical and structural changes to the actin cytoskeleton required for efficient migration.

Overall our data indicate that vinculin translocation between cell–cell and cell–ECM adhesions is an essential process in the homeostasis of the epithelium. Increased vinculin recruitment to cell–cell adhesions may not only strengthen cell–cell adhesions (Huveneers and de Rooij, 2013) but also appears to destabilize cell–ECM adhesions. It is tempting to speculate that vinculin translocation in itself is sufficient to drive transitions between a cortical-dominated actin stress fiber network to a stress-fiber dominated network (Chalut and Paluch, 2016).

METHODS

Request a protocol through *Bio-protocol*.

Cell culture

MDCK II cells were cultured in DMEM medium supplemented with 10% fetal bovine serum (FBS) and 1% penicillin-streptomycin (PS) at 37°C with 5% CO_2.

To generate α-catenin knockout cells, CRISPR/Cas9 was used (gRNA sequence: TCTGGCAGTTGAAAGACTGT in the Sigma into All-in-One U6-gRNA/CMV-Cas9-tGFP Vector). This gRNA sequence was previously shown to be effective in the knockout of canine α-catenin (Ozawa, 2018). Cells were transiently transfected with this

vector, followed by clonal expansion. Clones were screened for α-catenin loss using Western blotting.

To develop mutant rescue α-catenin cell lines, we developed mCherry N-terminally tagged versions of wild-type (available as Addgene plasmid 178646), L344P (available as Addgene plasmid 178647), and M319G/R326E (constitutively active or CA, available as Addgene plasmid 178648) using the pmCherryC1 vector (Clonetech). Human sequences for pGEX4T1 wild-type and L344P α-catenin were a kind gift of Kris DeMali (Peng *et al.*, 2012) and were subcloned from pGEX4T1 plasmids into pmCherryC1. A human α-catenin sequence containing the previously identified M319G/R326E mutations (Matsuzawa *et al.*, 2018) was synthetically cloned by GeneArt Gene Synthesis (ThermoFisher) and subsequently subcloned into pmCherryC1. These vectors were transiently transfected into α-catenin KO MDCK cells, followed by G418 selection (500 μg/ml for 7 d). Cells expressing high levels of mCherry fluorescence were manually selected using cloning rings.

Additional mCherry α-catenin cell lines were generated overexpressing vinculin. Lentivirus was generated using a pRRL vinculin-venus plasmid (gift of Brenton Hoffman), which contains chicken vinculin with a C-terminal venus fluorescent tag. Wild-type, CA, and L344P cells were infected, and positive cells were isolated using fluorescent cell sorting. Western blotting for vinculin was used to confirm overexpression (expression of both endogenous and fluorescently tagged vinculin).

Western blotting

Cells were washed with phosphate-buffered saline (PBS) and lysed using RIPA buffer supplemented with protease and phosphatase inhibitors. Standard SDS–PAGE and Western blotting techniques were performed using PDVF membranes. Resulting membranes were then incubated in 5% bovine serum albumin (BSA) PBS for 1 h at room temperature before being incubated overnight in primary antibody solution in 5% BSA PBS. The following day, samples were rinsed in 0.2% Tween PBS and incubated for 45 min with HRP secondary antibody in 0.2% Tween-100× PBS. Samples were rinsed with PBS and imaged using chemiluminescence using a Bio-Rad ChemiDoc system. Primary antibodies used for Western blotting were anti-rabbit α-catenin (Sigma, catalogue# C2081), vinculin (clone hVIN-1, Sigma), and anti-mouse tubulin (clone DM1A, Cell Signaling).

Immunofluorescence

Thirty-five-mm glass-bottom dishes (CellVis) were coated with bovine fibronectin (Sigma) for 15 min. Dishes were then washed with PBS and seeded with cells. After overnight incubation, cells were fixed with 2% paraformaldehyde for 15 min at room temperature and then permeabilized with 0.5% Triton X-100 in PBS for 20 min at room temperature. Cells were then incubated in 5% BSA PBS for 1 h at room temperature before being incubated overnight in primary antibody in 5% BSA PBS. The following day, cells were rinsed in PBS and incubated for 45 min with secondary antibodies in PBS. Cells were rinsed in PBS and incubated with Hoechst 33342 (ThermoFisher) diluted 1:10000 in PBS. Cells were mounted in 40 μl Prolong Gold Antifade. Fluorescent imaging was performed using either a Zeiss 710 LSM confocal microscope and a Zeiss 980 LSM confocal microscope with Airyscan.

The following antibodies were used for immunofluorescence assays: anti-mouse vinculin (clone hVIN-1, Sigma, Catalog #V9131), anti-rabbit vinculin (clone EPR8185, Abcam, Catalog #ab129002), anti-mouse paxillin (Clone 117, BD Catalog #610568), and anti-rabbit E-cadherin (Clone 24E10, Cell Signaling Catalogue #3195S). Alexa Fluor–conjugated secondary antibodies (ThermoFisher) were used in all staining experiments.

Quantification of vinculin recruitment to AJs was performed as described (Heier *et al.*, 2021). FA identification in immunostained images was performed as described (Horzum *et al.*, 2014) using vinculin as a marker of FAs. FAs could not be detected above cytoplasmic signal with paxillin and talin labeling. Optimization to achieve optimal identification of vinculin labeled FAs resulted in a size threshhold of 80 pixels, or 0.161 μm^2. To account for false-positive FA labeling resulting from vinculin signal at cell–cell contacts, identification of FAs was omitted from cell–cell contact regions as defined by a mask generated with a threshhold of mCherry α-catenin signal (Supplemental Figure S2). ImageJ was used to quantify number of FAs per cell and per area.

Calcium depletion assay

Thirty-five-mm glass-bottom dishes CellVis were coated with bovine fibronectin (Sigma) for 15 min. Dishes were then washed with PBS and seeded with $0.65 * 10^6$ cells. After overnight incubation, cells were rinsed six times with calcium/FBS free media (DMEM without calcium, ThermoFisher). Cells were then incubated in either calcium/FBS free media or regular media without FBS for 24 h. Following this 24 h period, cells were fixed and stained as normal.

Collective cell migration assay

Cells were seeded in ibidi Culture-Insert 2 Well in 35-mm μ-dishes and incubated overnight. The culture-insert well was removed the next day and 2 ml of DMEM medium supplemented with 5% FBS and 1% PS was added to each dish. Three different cell-free areas between the migrating colonies per dish were imaged every 2 h for 6 h. ImageJ was used to quantify the reduction in cell-free area over time. This area reduction was divided by the length of the frame to calculate migration rate. Migration rates were then normalized against α-catenin WT cells.

Time-lapse imaging was performed using a Zeiss 980 LSM confocal microscope with Airyscan at 37°C. Filamentous actin was labeled using SiR-actin (Cytoskeleton).

Preparation of substrates for traction force microscopy

Soft silicone (Qgel from CHT USA Inc, Cassopolis, MI) was prepared by mixing Qgel 300A and Qgel 300B in a ratio of 1: 2.2 by weight. 0.1 g of this Qgel mixture was pipetted onto a 22 × 22-mm glass coverslip (no. 1.5) and cured using a hot plate at 100°C for 1 h. Then, the cured silicone substrate was exposed to 305 nm UV light (UVP cross-linker, Analytik Jena AG, Upland, CA) for 5 min. The substrate was then incubated with a solution consisting of 10 mg/ml EDC (1-ethyl-3-(3-dimethylaminopropyl) carbodiimide hydrochloride), 5 mg/ml sulfo-NHS (N-hydroxysulfosuccinimide), 1 mg/ml fibronectin (Millipore Sigma, Burlington, MA), and 0.65 mg/ml red fluorescent beads of diameter 0.44 μm (Spherotech Inc., Lake Forest, IL) for 30 min at room temperature; afterward, the sample was washed two times with PBS and then used for plating cells. The silicone substrate's Young's modulus was determined to be 8.7 kPa as determined by shear rheology using an Anton Paar MCR 302 rheometer.

Imaging for traction force measurements

Phase images and bead images were obtained using a Leica DMi8 epifluorescence microscope (Leica Microsystems, Buffalo Grove, IL) consisting of a 10 × 0.3 NA objective, a Clara cooled CCD camera (Andor Technology, Belfast, Northern Ireland), and an airstream incubator (Nevtek, Williamsville, VA). The "cell off" bead image

(reference bead image of the substrate top surface) was obtained after releasing the cells off the substrate with 0.5% SDS.

Data analysis for and after traction force microscopy

The "cell on" and "cell off" bead images were aligned using Image J (Martiel *et al.*, 2015) and the bead displacement was then calculated using MATLAB (MathWorks, Natick, MA) as before (Sabass *et al.*, 2008; Dumbali *et al.*, 2017). From the displacement field, traction force reconstruction was performed using Fourier transform traction cytometry that uses the Boussinesq solution (Sabass *et al.*, 2008; Maruthamuthu and Gardel, 2014). The total frequency (number of traction data points) considered for the two cases (MDCK and MDCK α-cat KO with CA α-cat) was equalized by normalizing the total frequency of traction magnitudes for MDCK by the ratio of the total area of MDCK islands to that of islands of MDCK α-cat KO with CA α-cat (obtained by manual segmentation using ImageJ [Collins, 2007]). The traction stress magnitudes above background (> 50 Pa) were selected and plotted using Mathematica (Wolfram Research, Champaign, IL).

ACKNOWLEDGMENTS

We acknowledge Kris DeMali and Brenton Hoffman for generously providing reagents used in this work. Additionally, we acknowledge helpful discussions with Kris DeMali, Cara Gottardi, Brenton Hoffman, Uktu Horzum, and Adam Kwiatkowski during the course of this project. This work was supported by NIH administrative supplement R35GM119617-05S1 (to V.B.-P.), NIH Grant R35 GM119617 (to D.C.), NIH Grant R15 GM116082 (to V.M.), and NSF CAREER award CMMI 1653299 (to D.C.) Services in support of the research project were generated by the VCU Massey Cancer Center Flow Cytometry Shared Resource in part with funding from NIH-NCI Cancer Center Support Grant P30 CA016059.

REFERENCES

Bays JL, DeMali KA (2017). Vinculin in cell–cell and cell–matrix adhesions. Cell Mol Life Sci 74, 2999–3009.

Campbell ID, Humphries MJ (2011). Integrin structure, activation, and interactions. Cold Spring Harb Perspect Biol 3, 1–14.

Carisey A, Tsang R, Greiner AM, Nijenhuis N, Heath N, Nazgiewicz A, Kemkemer R, Derby B, Spatz J, Ballestrem C (2013). Vinculin regulates the recruitment and release of core focal adhesion proteins in a force-dependent manner. Curr Biol 23, 271–281.

Chalut KJ, Paluch EK (2016). The actin cortex: A bridge between cell shape and function. Dev Cell 38, 571–573.

Collins TJ (2007). ImageJ for microscopy. Biotechniques 43, S25–S30.

Dumbali SP, Mei L, Qian S, Maruthamuthu V (2017). Endogenous sheet-averaged tension within a large epithelial cell colony. J Biomech Eng 139, 1010081–1010085.

Gallant ND, Michael KE, García AJ (2005). Cell adhesion strengthening: contributions of adhesive area, integrin binding, and focal adhesion assembly. Mol Biol Cell 16, 4329.

Geiger B, Yamada KM (2011). Molecular architecture and function of matrix adhesions. Cold Spring Harb Perspect Biol 3, 1–21.

Gomez EW, Chen QK, Gjorevski N, Nelson CM (2010). Tissue geometry patterns epithelial-mesenchymal transition via intercellular mechanotransduction. J Cell Biochem 110, 44–51.

Heier JA, Pokutta S, Dale IW, Kim SK, Hinck AP, Weis WI, Kwiatkowski AV. (2021). Distinct intramolecular interactions regulate autoinhibition of vinculin binding in αT-catenin and αE-catenin. J Biol Chem 296, 100582.

Horzum U, Ozdil B, Pesen-Okvur D (2014). Step-by-step quantitative analysis of focal adhesions. MethodsX 1, 56–59.

Humphries JD, Wang P, Streuli C, Geiger B, Humphries MJ, Ballestrem C (2007). Vinculin controls focal adhesion formation by direct interactions with talin and actin. J Cell Biol 179, 1043–1057.

Huttenlocher A, Horwitz AR (2011). Integrins in cell migration. Cold Spring Harb Perspect Biol 3, 1–16.

Huveneers S, de Rooij J (2013). Mechanosensitive systems at the cadherin-f-actin interface. J Cell Sci 126, 403–413.

Koirala R, Priest AV, Yen CF, Cheah JS, Pannekoek WJ, Gloerich M, Yamada S, Sivasankar S (2021). Inside-out regulation of E-cadherin conformation and adhesion. Proc Natl Acad Sci USA 118.

Martiel JL, Leal A, Kurzawa L, Balland M, Wang I, Vignaud T, Tseng Q, Théry M (2015). Measurement of cell traction forces with ImageJ. Methods Cell Biol 125, 269–287.

Maruthamuthu V, Gardel ML (2014). Protrusive activity guides changes in cell-cell tension during epithelial cell scattering. Biophys J 107, 555–563.

Matsuzawa K, Himoto T, Mochizuki Y, Ikenouchi J (2018). α-Catenin controls the anisotropy of force distribution at cell-cell junctions during collective cell migration. Cell Rep 23, 3447–3456.

Mertz AF, Che Y, Banerjee S, Goldstein JM, Rosowski KA, Revilla SF, Niessen CM, Marchetti MC, Dufresne ER, Horsley V (2013). Cadherin-based intercellular adhesions organize epithelial cell–matrix traction forces. Proc Natl Acad Sci USA 110, 842–847.

Monster JL, Donker L, Vliem MJ, Win Z, Matthews HK, Cheah JS, Yamada S, de Rooij J, Baum B, Gloerich M (2021). An asymmetric junctional mechanoresponse coordinates mitotic rounding with epithelial integrity. J Cell Biol 220, e202001042.

Mui KL, Chen CS, Assoian RK (2016). The mechanical regulation of integrin-cadherin crosstalk organizes cells, signaling and forces. J Cell Sci 129, 1093–1100.

Narayanan V, Schappell LE, Mayer CR, Duke AA, Armiger TJ, Arsenovic PT, Mohan A, Dahl KN, Gleghorn JP, Conway DE (2020). Osmotic gradients in epithelial acini increase mechanical tension across E-cadherin, drive morphogenesis, and maintain homeostasis. Curr Biol 30, 624–633.e4.

Noethel B, Ramms L, Dreissen G, Hoffmann M, Springer R, Rübsam M, Ziegler WH, Niessen CM, Merkel R, Hoffmann B (2018). Transition of responsive mechanosensitive elements from focal adhesions to adherens junctions on epithelial differentiation. Mol Biol Cell 29, 2317–2325.

Ozawa M (2018). Nonmuscle myosin IIA is involved in recruitment of apical junction components through activation of α-catenin. Biol Open 7, bio031369.

De Pascalis C, Etienne-Manneville S (2017). Single and collective cell migration: the mechanics of adhesions. Mol Biol Cell 28, 1833–1846.

Peng X, Maiers JL, Choudhury D, Craig SW, DeMali KA (2012). α-Catenin uses a novel mechanism to activate vinculin. J Biol Chem 287, 7728–7737.

Del Rio A, Perez-Jimenez R, Liu R, Roca-Cusachs P, Fernandez JM, Sheetz MP (2009). Stretching single talin rod molecules activates vinculin binding. Science (80-) 323, 638–641.

Sabass B, Gardel ML, Waterman CM, Schwarz US (2008). High resolution traction force microscopy based on experimental and computational advances. Biophys J 94, 207–220.

Sakakibara S, Mizutani K, Sugiura A, Sakane A, Sasaki T, Yonemura S, Takai Y (2020). Afadin regulates actomyosin organization through αE-catenin at adherens junctions. J Cell Biol 219, e201907079.

Scott LE, Griggs LA, Narayanan V, Conway DE, Lemmon CA, Weinberg SH (2020). A hybrid model of intercellular tension and cell–matrix mechanical interactions in a multicellular geometry. Biomech Model Mechanobiol 19, 1997–2013.

Seddiki R, Narayana GHNS, Strale PO, Balcioglu HE, Peyret G, Yao M, Le AP, Teck Lim C, Yan J, Ladoux B, *et al.* (2018). Force-dependent binding of vinculin to α-catenin regulates cell-cell contact stability and collective cell behavior. Mol Biol Cell 29, 380–388.

Sumida GM, Tomita TM, Shih W, Yamada S (2011). Myosin II activity dependent and independent vinculin recruitment to the sites of E-cadherin-mediated cell-cell adhesion. BMC Cell Biol 12, 1–9.

Vasquez CG, Martin AC (2016). Force transmission in epithelial tissues. Dev Dyn 245, 361–371.

Weber GF, Bjerke MA, DeSimone DW (2012). A mechanoresponsive cadherin-keratin complex directs polarized protrusive behavior and collective cell migration. Dev Cell 22, 104–115.

Yang Y-A, Nguyen E, Narayana G, Heuzé M, Fu C, Yu H, Mège R-M, Ladoux B, Sheetz MP (2022). Local contractions regulate E-cadherin rigidity sensing. Sci Adv 8, 387.

Yao M, Qiu W, Liu R, Efremov AK, Cong P, Seddiki R, Payre M, Lim CT, Ladoux B, Mège RM, *et al.* (2014). Force-dependent conformational switch of α-catenin controls vinculin binding. Nat Commun 2014 51 5, 1–12.

Yonemura S, Wada Y, Watanabe T, Nagafuchi A, Shibata M (2010). α-Catenin as a tension transducer that induces adherens junction development. Nat Cell Biol 12, 533–542.

Zhou DW, Lee TT, Weng S, Fu J, García AJ (2017). Effects of substrate stiffness and actomyosin contractility on coupling between force transmission and vinculin-paxillin recruitment at single focal adhesions. Mol Biol Cell 28, 1901–1911.